Research Square

Preprints are preliminary reports that have not undergone peer review.
They should not be considered conclusive, used to inform clinical practice,
or referenced by the media as validated information.

Hybrid Fabrication of Patient-Specific Intraoral Stents for Head and Neck Radiotherapy: A Retrospective Case Series with Exploratory Dosimetry

Anna Dovhan

dovgananna04@gmail.com

Educational and Research Institute of Dentistry, Bogomolets National Medical University

Olena Bakhmatska

National Cancer Institute

Denys Sliusarenko

National Cancer Institute

Nadiia Yaroshenko

National Cancer Institute

Maryna Sokolovska

National Cancer Institute

Oleg Kravets

National Cancer Institute

Ruben Del Castillo Pacora

Kingston Health Sciences Centre

Roman Palyvoda

Educational and Research Institute of Dentistry, Bogomolets National Medical University

Rodrigo Salazar-Gamarra

Universidad Peruana Cayetano Heredia

Dmytro Filonenko

Kyiv Regional Clinical Hospital

Research Article

Keywords: patient-specific intraoral positioning stent, maxillofacial prosthetics, radiotherapy, head and neck tumors, digital dentistry, three-dimensional printing, dosimetry

Posted Date: November 10th, 2026

DOI: https://doi.org/10.21203/rs.3.rs-11598838/v1

License: This work is licensed under a Creative Commons Attribution 4.0 International License.
Read Full License

Additional Declarations: No competing interests reported.

Hybrid Fabrication of Patient-Specific Intraoral Stents for Head and Neck Radiotherapy: A Retrospective Case Series with Exploratory Dosimetry

Anna Dovhan[1,2,*], Olena Bakhmatska[3], Denys Sliusarenko[3], Nadiia Yaroshenko[4], Maryna Sokolovska[5], Oleg Kravets[6], Ruben Del Castillo Pacora[7], Roman Palyvoda[8], Rodrigo Salazar-Gamarra[9,10], Dmytro Filonenko[2,8]

1 Educational and Research Institute of Dentistry, Bogomolets National Medical University, Kyiv, Ukraine.

2 Center for Head and Neck Pathology, Kyiv Regional Clinical Hospital, Kyiv, Ukraine.

3 Center for Radiology and Radiation Therapy, National Cancer Institute, Kyiv, Ukraine.

4 Department of Radiation Therapy, National Cancer Institute, Kyiv, Ukraine.

5 Center for Radiation Oncology, National Cancer Institute, Kyiv, Ukraine.

6 Research and Clinical Department of Head and Neck Tumors, National Cancer Institute, Kyiv, Ukraine.

7 Department of Oncology, Kingston Health Sciences Centre, Kingston, Ontario, Canada.

8 Department of Maxillofacial Surgery, Educational and Research Institute of Dentistry, Bogomolets National Medical University, Kyiv, Ukraine.

9 "Unidad de Innovación y Desarrollo en Estomatología" at "Universidad Peruana Cayetano Heredia", Lima, Peru.

10 "Instituto Mais Identidade", São Paulo, Brazil.

* Corresponding author: Anna Dovhan, dovgananna04@gmail.com

Abstract

Background

Patient-specific intraoral positioning stents enable targeted positioning of the jaws and soft tissues during radiotherapy for head and neck tumors. Combining functional molding with digital manufacturing extends the

scope for adaptation to the patient's dental status, including complete edentulism and postoperative anatomical changes. This study aimed to present a hybrid stent fabrication workflow and evaluate its clinical application and effects on the calculated dose distribution.

Methods

A retrospective descriptive case series examined fabrication and clinical use of individualized intraoral stents in 16 adults with head and neck tumors. Functional silicone templates were molded intraorally, digitized by extraoral optical scanning, and reproduced in polylactic acid by three-dimensional printing. Manufacturing and clinical records were reviewed descriptively. Whole oral-cavity mean dose was evaluated in seven paired comparisons with and without the stent. Serial sagittal kV-CBCT images from three illustrative patients were assessed qualitatively.

Results

Patient-specific intraoral positioning stents were used for caudal tongue displacement in 13 patients, lip retraction in two, and cheek retraction in one. Two patients were completely edentulous in both jaws. Whole oral-cavity Dmean decreased in five of seven paired comparisons; the average decreased from 44.11 to 42.94 Gy, a mean paired reduction of 1.17 Gy. The largest reduction was 5.2 Gy (9.3%) in patient 12, whose uninvolved oral-cavity Dmean also decreased by 3.3 Gy (7.3%). Reported PTV coverage was unchanged in all three detailed pairs. Dose changes in other organs were heterogeneous, including increases in selected structures. Serial images showed broadly similar jaw opening and tongue–palate separation across the illustrated fractions. Eleven patients completed radiotherapy with the stent. No device breakage or intolerance was reported; one stent was reworked before treatment for comfort.

Conclusions

The hybrid workflow enabled individualized tissue positioning across diverse dental and postoperative conditions, including complete edentulism. The paired comparisons support a selective dosimetric benefit: lower average oral-cavity exposure in most evaluated pairs, with no decline in reported target coverage in the three detailed comparisons. These findings, together with the illustrated anatomical separation and clinical

usability, support prospective evaluation of patient-specific stents as an adjunct to treatment planning. Reduced clinical toxicity and superiority over independently optimized plans were not established.

Keywords: patient-specific intraoral positioning stent; maxillofacial prosthetics; radiotherapy; head and neck tumors; digital dentistry; three-dimensional printing; dosimetry.

Background

Radiotherapy for head and neck tumors requires adequate target dose coverage while limiting irradiation of adjacent healthy tissues. The anatomical proximity of the tongue, palate, cheeks, lips, and salivary glands to the tumor or postoperative bed creates a need for patient-specific spatial separation of these structures. Intraoral stents allow the required tissue relationships to be established during treatment planning [1]. Device design is determined by the target location, the intended direction of displacement, and the anatomical conditions available for support.

Positioning stents maintain the jaws and soft tissues in a defined configuration and, depending on the clinical objective, provide tongue depression or lateralization, lip retraction, or cheek retraction [2]. In the present series, the devices were used for caudal tongue displacement and retraction of the lips or cheek away from the dentoalveolar arch. The dosimetric effect of this approach is primarily associated with changes in the spatial relationship between the tissues, the target, and the dose distribution.

Customization of the supporting surfaces is particularly important in patients with partial or complete tooth loss and postoperative anatomical changes. When the dentition is preserved, its contours provide landmarks for stent placement. In edentulous patients or after resection, support is designed around the alveolar regions, mucosa, and reconstructed tissues. The use of dental and alveolar support highlights the role of clinical fitting in the development of a patient-specific intraoral positioning stent [1].

Digital technologies allow anatomical data to be transferred to a virtual model and subsequently used to manufacture a stent by three-dimensional printing. Published approaches involve diagnostic computed tomography (CT) imaging, optical scanning, or clinical adaptation of prefabricated devices [2, 3, 4]; digital and manual methods have also been compared in clinical studies [5]. Our proposed hybrid workflow begins

with chairside functional molding of a silicone pattern directly within the oral cavity. This pattern provides the geometry for stent design and is subsequently scanned extraorally for digital modeling and three-dimensional printing. The fabrication pathway does not require direct scanning of the patient's jaws or involvement of an external dental laboratory, supporting a mobile clinical workflow with access to an optical scanner and a 3D printer. In the study by Li et al. [5], 12 patients were compared using 3D-printed and conventional stents; oral-cavity mean doses were 33.31 and 34.72 Gy, respectively ($P = 0.15$), and reported fabrication times were 4.5 ± 0.5 and 25.2 ± 2.4 h. These different workflows and endpoints do not establish equivalence or permit direct comparison of their total fabrication times with the printer run times reported here.

Bruno et al. designed a stent from a direct intraoral scan in a patient with tongue cancer and compared calculated doses on planning scans with and without the appliance [6]. Dağdelen et al. evaluated a printed positioning stent specifically for edentulous patients [7]. In our workflow, a removable silicone pattern records how the selected teeth, ridge, or reconstructed mucosa support the stent while the target tissue position is established. The pattern is then scanned outside the mouth.

This study aimed to describe a hybrid workflow for fabricating patient-specific intraoral positioning stents and to evaluate its application in terms of anatomical adaptation, fabrication characteristics, and dosimetric changes. The multidisciplinary approach integrates the expertise of a prosthodontist, a radiation oncologist, and a medical physicist. An additional objective was to illustrate stent seating and maintenance of the intended tissue configuration across selected treatment fractions.

Methods

Study Design and Data Sources

A retrospective descriptive study was conducted in a series of 16 adult patients with head and neck tumors entered into the clinical registry of the Department of Radiation Therapy, National Cancer Institute, Kyiv, Ukraine, with patient inclusion from June to October 2026. The patient was the unit of the descriptive case series; device variants and paired imaging studies were considered within the corresponding clinical case. Recorded multidisciplinary consultation dates ranged from 8 July to 23 September 2026. These dates are distinguished from the subsequent radiotherapy and follow-up dates. Patients were considered for stent

fabrication when the radiation oncologist identified a need for tongue positioning or lip or cheek retraction. Exclusion criteria for device use were severe pain, a pronounced gag reflex, and psychiatric disorders, as specified by the clinical team. Characteristics of the series and individual treatment records are summarized in Tables 1 and 2.

The study documentation included clinical records and complete photographic documentation for all 16 patients. Dental and clinical characteristics, tissue positioning objectives, and stent fabrication parameters were analyzed. Whole oral-cavity mean dose analysis included seven paired comparisons within the series; geometric features were assessed using CT images with linear measurements and isodose displays. The most illustrative photographs were selected for publication to demonstrate fabrication stages, design solutions, and device application. These selected images form part of the complete documentation for the clinical series. The three detailed dosimetric comparisons comprise registry patients 1, 2, and 12.

Patients are identified by study numbers 1-16. The detailed dosimetric pairs 1, 2 and 3 correspond to patients 1, 2 and 12, respectively. Seven patients had paired whole oral-cavity mean dose measurements. Three patients were selected to illustrate serial imaging and are identified separately as S1–S3.

Dental Assessment and Template Molding

The radiation oncologist defined the clinical objective, specifying the structure to be displaced, the direction of displacement, and the position to be stabilized. Dental examination included assessment of the remaining teeth, retained roots, dental prostheses, edentulous regions, oral mucosa, and postoperative changes. These findings determined the configuration of the supporting surfaces and the path of stent insertion.

A functional template was molded directly in the oral cavity using condensation silicone (C-silicone) impression material to register the intended jaw relationship and soft tissue position. Tooth contours were reproduced in dentate regions, whereas the available alveolar contours and mucosal surfaces were recorded in edentulous regions. The template was digitized extraorally using a Medit i600 intraoral optical scanner. The resulting geometry served as the basis for the digital design of the final device. The silicone pattern itself was the scanned design input; direct scanning of the patient’s jaws and an external dental laboratory were not required for this fabrication workflow. The fabrication sequence is illustrated in Figure 1.

Fit and mandibular stabilization were assessed clinically by evaluating whether the stent returned to its defined supporting position on reinsertion and restricted visible lateral and anterior mandibular movements. Tissue relationships were also assessed on planning CT images.

Assessment of Stent Seating and Tissue Position

Reproducibility was considered at two levels: return of the stent to its supporting position after reinsertion, and maintenance of the intended jaw and soft tissue configuration during repeated use. Clinical assessment of reinsertion was complemented by a qualitative review of 12 sagittal images from three illustrative patients (S1–S3), with four images per patient documented for fractions 1, 10, 28, and 30. The visible jaw relationship, oral opening, and tongue–palate separation were compared within each set. The serial sagittal images were obtained from kilovoltage cone-beam CT (kV-CBCT).

The serial images were reviewed separately from the paired dosimetric comparisons. Interfraction positioning was assessed qualitatively at the documented fractions 1, 10, 28, and 30.

Digital Fabrication

Digital design was performed in Meshmixer version 3.5.474. During this stage, contact surfaces and undercuts were smoothed, occlusal indentations and lingual and lateral support areas were refined, and a through-channel for breathing was incorporated. The digital model was retained to allow potential refabrication, provided that the anatomy of the supporting tissues remained unchanged.

Stents were fabricated from polylactic acid (PLA) using fused deposition modeling (FDM). According to the manufacturing documentation, Bambu Lab PLA Pure material and a Bambu Lab X2D printer were used. The printing profile specified a layer height of 0.12 mm, an initial layer height of 0.20 mm, two wall perimeters, five top and five bottom solid layers, and 8% gyroid infill. The outer wall printing speed was 60 mm/s, and the infill speed was 150 mm/s. The recommended temperature ranges for the material were 190–230 °C for the nozzle and 35-65 °C for the build plate. The same printer and unchanged 0.12 mm High Quality profile were used across cases. Material documentation included SGS reports CANEC26004736501, CANEC26004736503, and CANEC26004736505 (11 March 2026), reporting that orange, pink, and white

PLA Pure samples, respectively, passed EN 71-3:2019+A2:2024 testing for migration of certain elements. The documentation also listed UL GREENGUARD certificate 429084-410 (23 March 2026–23 March 2027).

Manufacturing characteristics were assessed using print job duration and stent mass. Fourteen single-device print jobs were summarized separately from two batch jobs, each producing two design variants simultaneously. The duration of a batch job was not treated as the printing time of one device. The reported clinical workflow spanned three days from silicone pattern fabrication to delivery and fitting of the stent. On day 1, the silicone pattern was formed intraorally, scanned extraorally, and used for digital modeling. Printing and sterilization were performed on day 2. On day 3, the stent was fitted to the patient and adjusted for comfort as needed before delivery for clinical use. This three-day turnaround describes the clinical schedule and is distinct from printer run time and hands-on operator time. Printing times and masses are reported in the manufacturing table (Table 3).

Sterilization

Following fabrication, completion of post-processing, and cleaning, each patient-specific intraoral radiotherapy stent underwent a single cycle of low-temperature hydrogen peroxide (H_2O_2) gas-plasma sterilization in a STERRAD 100NX system (Advanced Sterilization Products), using the STANDARD cycle, before its first insertion into the patient's oral cavity. In addition to initial fitting and any comfort adjustments before radiotherapy, intraoral contact occurred during radiotherapy treatment sessions. Adjustments were performed at initial fitting. Between fractions, stents were washed with water and stored in dry conditions with continuous air circulation, away from direct sunlight, heat sources, and access by animals.

Dosimetric Comparison

Paired dosimetric comparisons were performed using CT datasets acquired with an intraoral positioning stent (CT1) and without the stent (CT2). Both CT scans were acquired during the same simulation session at an interval of approximately 5 minutes, using a tube voltage of 120 kV and a slice thickness of 1 mm. The patient remained in the initial immobilization setup without repositioning between scans, allowing the treatment isocenter to be maintained at the same coordinates.

Treatment planning was performed using the Monaco treatment planning system (version 6.2.2, Elekta) for an Elekta Harmony linear accelerator with 6 MV photon beams. Volumetric modulated arc therapy (VMAT) was used, and dose distributions were calculated using the X-ray Voxel Monte Carlo (XVMC) algorithm with a dose calculation grid resolution of 0.3 cm (3 mm) and a statistical uncertainty setting of 1%.

The initial treatment plan was optimized on CT1 (with the stent) and subsequently recalculated on CT2 (without the stent), without reoptimization or changes to the radiation delivery parameters. The treatment isocenter, beam geometry, multileaf collimator configurations, monitor units, and plan normalization remained unchanged. This approach enabled comparison of the calculated dose distributions under different anatomical conditions while maintaining identical irradiation parameters. This fixed-plan recalculation assesses dose redistribution under unchanged delivery parameters; it does not compare two independently optimized clinical plans.

The two CT datasets were registered using bony anatomical landmarks. A radiation oncologist performed contouring of the planning target volume (PTV) and organs at risk (OARs). Contours were transferred between the registered images, followed by visual review and manual adjustment by the radiation oncologist to account for anatomical differences associated with stent use. Consequently, PTV volumes were comparable but not identical between the two configurations because of differences in anatomical geometry.

The dosimetric analysis reported nine dose parameters for the entire oral cavity, its uninvolved portion, the ipsilateral and contralateral parotid and submandibular glands, the lips, and the mandible (Table 4). Mean dose (Dmean) and maximum dose (Dmax) were determined from the treatment planning system data. The uninvolved oral cavity was generated by Boolean subtraction of the PTV from the entire oral cavity (oral cavity minus PTV).

PTV coverage was assessed using V95% and V100%, defined as the percentages of the PTV receiving at least 95% and 100% of the prescribed dose, respectively. The conformity index (CI) and homogeneity index (HI) were also recorded. CI and HI were obtained directly from the automatic calculations in the Monaco treatment planning system (version 6.2.2).

The conformity index was calculated automatically in Monaco using the Paddick formula [8] at a reference isodose of 95% of the prescribed target dose: $CI_95 = (TV_95)^2 / (TV \times V_95)$, where TV is the PTV, V_95 is the total volume receiving at least 95% of the prescribed target dose, and TV_95 is the portion of the PTV within that isodose volume. The index is dimensionless, ranges from 0 to 1, and has an ideal value of 1. The reference dose was specified through the Prescribed Dose parameter in the dose–volume histogram (DVH) statistics; this evaluation setting is distinct from the clinical treatment prescription. The same 95% reference level was used for all six configurations: 62.7 Gy for pairs 1 and 2 (66-Gy prescriptions) and 66.5 Gy for pair 3 (70-Gy prescription).

The homogeneity index was calculated automatically by the treatment planning system (TPS) as HI_ratio = D2% / D98%, where D2% and D98% are the doses received by at least 2% and 98% of the PTV, respectively (near-maximum and near-minimum target doses). This dimensionless ratio has an ideal value of 1, with larger values indicating greater heterogeneity. It differs from the ICRU Report 83 index [9], $HI_ICRU83 = (D2\% - D98\%) / D50\%$, for which 0 is ideal and D50% is the median target dose. The HI values reported in this study use the D2%/D98% definition.

The study medical physicist verified the reported dosimetric values against the source treatment-planning records and confirmed the index definitions and reference-dose settings. CI_95 was interpreted alongside V95%, which describes target coverage at the same dose threshold. In general, $CI_95 \leq TV_95/TV = V95\%/100$; with V95% = 100%, CI_95 reduces to TV/V_95. V100% describes target coverage at a separate dose threshold.

Three regions of the stent were measured on CT, and the mean and standard deviation of the CT values were recorded in Hounsfield units (HU). Linear distances from the midpoint of the bony hard palate to the target location on sagittal planning CT were recorded in millimeters. These distances describe anatomy and do not directly measure mucosal dose.

Descriptive Analysis

Quantitative variables were summarized using the median, first and third quartiles, and range. Quartiles were calculated by linear interpolation. Demographic, anatomical, and fabrication characteristics were described for the overall series of 16 patients.

The paired difference was calculated as the value with the stent minus the value without the stent. Dose changes were expressed in gray, and changes in V95% and V100% in percentage points. The relative dose change was calculated by dividing the paired difference by the dose without the stent and multiplying by 100%. Thirteen parameters were described for each of the initial three pairs. For the entire oral cavity, arithmetic means of Dmean with and without the stent and the mean paired difference were calculated across all seven pairs; the analysis was descriptive.

Results

Patient and Dental Characteristics

The clinical series comprised nine men and seven women. The median age was 56.5 years, with first and third quartiles of 51.5 and 74.0 years and a range of 41-79 years. Tumor sites included the base and lateral surface of the tongue, the floor of the mouth, the lower lip, and the buccal mucosa. Six patients had previously undergone oncological surgery.

In 13 of the 16 patients, the stent was intended for caudal tongue displacement, in two for lip retraction, and in one for cheek retraction. Two patients were completely edentulous in both jaws. Twelve patients had remaining teeth in both jaws; in one case, an edentulous maxilla was combined with individual remaining teeth or restorations in the mandible. In another case, the supporting conditions were characterized by the status of the mandibular teeth and retained roots. The main characteristics of the series are presented in Table 1. Individual tumor diagnoses, histology, recorded TNM and stage, and treatment characteristics are presented in Table 2. The three detailed dosimetric pairs correspond, in order, to registry patients 1, 2, and 12: a patient with human papillomavirus (HPV)-unassociated base-of-tongue squamous cell carcinoma (SCC), a patient with HPV-associated base-of-tongue SCC, and a patient with surgically treated left lateral tongue SCC. The prescribed main-target doses for pairs 1 and 2 were 66 Gy in 33 fractions (2 Gy per fraction). For pair 3

(registry patient 12), the prescribed main-target dose was 70 Gy (Table 2). For patient 1, the multidisciplinary team (MDT) prescription was 66 Gy, and the stent was used in all 33 fractions. The positioning objective in all three cases was caudal tongue displacement. Tongue displacement, lip retraction, and cheek retraction represent three clinical applications of one fabrication workflow; their distinct positioning objectives should not be treated as a single uniform dosimetric intervention.

The hybrid workflow enabled sequential transfer of the functionally established configuration from the silicone template to the digital model and the printed stent (Figure 1). In patients with complete edentulism and postoperative changes, broad supporting surfaces were adapted to the available anatomical structures (Figure 2). These examples demonstrate the scope for device customization under challenging tissue support conditions.

According to the clinical records, 11 of 16 patients completed the radiotherapy course using the stent. No device breakage, device-related pain, or intolerance was reported. No pronounced gag reflex or trismus was reported during stent use in radiotherapy sessions. One stent was reworked before the start of radiotherapy to improve patient comfort. Fitting adjustments were required only at initial placement. Minimal tongue pressure was intentional where required by the radiation oncologist's positioning prescription. Stent use was discontinued in two patients: one died, and another discontinued radiotherapy because of peritonitis and pneumonia. These reports do not imply absence of radiotherapy-related mucosal symptoms. Treatment-course outcomes were summarized for 13 patients. The course status of the other three was not reported. No stent-related mucosal trauma was reported. No cases were reported in which mucositis prevented the patient from wearing the stent.

Printing Time and Device Mass

Printing parameters and stent mass are presented in Table 3. The 14 single-device print jobs had a median printing time of 153.5 min (range, 40-195 min). The two batch jobs, each producing two design variants simultaneously, took 200 and 230 min. The median stent mass was 21.0 g, with quartiles of 20.5 and 22.0 g and a range of 12.0-22.0 g.

The stent used to retract both lips had a mass of 15.0 g and was printed in 93 min; the cheek retraction stent had a mass of 12.0 g and was printed in 40 min. These durations describe the printing stage and do not represent the complete fabrication workflow.

Dose Distribution

Across seven paired comparisons, stent use was associated with a decrease in the average whole oral-cavity Dmean from 44.11 Gy without the stent to 42.94 Gy with the stent. The mean paired reduction was 1.17 Gy (approximately 2.7% of the mean without-stent dose). Dose decreased in five of the seven pairs, with a maximum individual reduction of 5.2 Gy. In one pair, the dose remained unchanged; in another, it increased by 0.9 Gy. The paired changes (with minus without the stent) were −0.6, −2.2, −5.2, +0.9, 0.0, −0.3, and −0.8 Gy, respectively. The paired changes are listed in Additional file 1 and plotted in Additional file 2.

In the three detailed pairs, contralateral parotid Dmean decreased by 1.6, 2.9, and 0.3 Gy. Pair 3 (registry patient 12; prescription, 70 Gy) showed the largest whole oral-cavity reduction: 56.2 to 51.0 Gy, a decrease of 5.2 Gy (9.3%). Uninvolved oral-cavity Dmean decreased from 45.3 to 42.0 Gy, a decrease of 3.3 Gy (7.3%), while its Dmax changed from 73.3 to 73.1 Gy. Ipsilateral and contralateral parotid Dmean also decreased, from 25.5 to 25.0 Gy and from 22.3 to 22.0 Gy, respectively. These favorable changes coexisted with an increase in ipsilateral submandibular Dmean from 65.7 to 70.0 Gy and mandibular Dmax from 72.0 to 73.0 Gy. The with-stent submandibular Dmean, uninvolved oral-cavity Dmax, and mandibular Dmax correspond to 100.0%, 104.4%, and 104.3% of the 70-Gy prescription, respectively. Across pairs 1–3, ipsilateral submandibular Dmean increased by 0.7, 0.3, and 4.3 Gy; mandibular Dmax increased by 1.3, 0.4, and 1.0 Gy. Uninvolved oral-cavity Dmean changed by 0.0, +1.7, and −3.3 Gy, and lip Dmean by +0.9, −1.2, and +2.4 Gy. Thus, the observed benefit was selective rather than uniform across organs. Table 4 presents the complete reported profile.

The recorded volumetric target coverage metrics were unchanged between configurations: PTV V95% was 100%, and PTV V100% was 90% under both conditions in all three pairs. The Paddick conformity index at the 95% reference isodose (CI_95) changed from 0.90 to 0.92, from 0.87 to 0.89, and from 0.89 to 0.90. These values are mathematically compatible with the reported V95% = 100% and indicate slightly greater

conformity of the 95% isodose volume with the stent in these descriptive comparisons. HI_ratio was 1.05 under both conditions in the first and third pairs and changed from 1.06 to 1.05 in the second. Under the D2%/D98% definition, these values indicate a near-maximum to near-minimum target dose ratio of 1.05–1.06, consistent with relatively homogeneous target dosing.

Mean CT values in the three measured regions of the stent were −804, −969, and −618 HU, with corresponding standard deviations of 500, 185, and 490 HU. These characteristics reflect the structure of the printed device, which combines polymer elements and air spaces. These region-of-interest measurements characterize the heterogeneous polymer–air structure rather than the intrinsic attenuation of solid PLA.

Figure 3 shows the four serial sagittal images from patient S1.

Planning CT geometry

In two paired planning CT examples, the palate-to-target distances without and with the stent were 17.8 and 30.7 mm in patient 1 and 7.5 and 15.1 mm in patient 12, respectively. These measurements describe anatomy at simulation. Figure 4 summarizes organ doses and target coverage across the three detailed dosimetric pairs. Figure 5 shows the paired isodose distributions in patient 12, whose whole oral-cavity mean dose decreased from 56.2 to 51.0 Gy (Table 4). The imaging appendix includes the other paired planning views from the same export (Additional file 3).

Reproducibility of Positioning

Sagittal cone-beam CT images were reviewed qualitatively for three illustrative patients at fractions 1, 10, 28 and 30. Jaw opening and tongue–palate separation appeared broadly similar across the reviewed fractions within each patient. Figure 3 shows one of the three cases.

Discussion

Clinical Customization and Digital Reproduction

The distinguishing feature of the proposed approach is a clinically led fabrication workflow that does not involve an external dental laboratory. A silicone pattern is formed directly in the patient’s mouth to establish the intended jaw relationship, soft tissue position, and supporting contours. Extraoral scanning of this pattern

provides the basis for digital stent design without direct scanning of the patient's jaws. The chairside pattern-making stage and the absence of a laboratory handoff support a mobile workflow that can be organized around available optical scanning and 3D-printing facilities. These are practical features of the fabrication pathway; comparative reductions in total production time or cost were not measured in this series.

Herpel et al. described the clinical adaptation of a preprinted device to the dentition using silicone material [2]. In our workflow, the patient-specific functional template is created before scanning and printing. This sequence transfers clinically defined supporting surfaces to the digital model without requiring segmentation of the dentition on CT. Planning CT is used to assess tissue relationships and dose distribution.

An important feature of this clinical series is the application of the method under different support conditions, including complete edentulism and postoperative anatomical changes. In these cases, the stent configuration was shaped according to the available alveolar and mucosal surfaces, extending the practical scope of patient-specific positioning. A further advantage is retention of the digital model for refabrication when the anatomy remains unchanged. Comparative assessment of fabrication time, accuracy, and economic parameters is planned for the next stage of the study.

In the lead-in phase of a multicenter trial, Tino et al. used direct intraoral scanning and stereolithographic fabrication. Fifteen of 18 enrolled patients received stents, and design and fabrication took an average of 8 h [10]. Their timing covers different stages from our interval between molding and clinical delivery, so it does not establish a difference in production speed. The prototype study in edentulous patients also used cone-beam CT to assess positioning [7]. Our two cases with complete edentulism illustrate how mucosal support can be incorporated during molding, but the series did not measure seating accuracy in this subgroup.

Dosimetric Potential of Patient-Specific Positioning

In the seven paired calculations, average oral-cavity exposure was lower with the stent. The reported target coverage metrics were unchanged in the three detailed comparisons. Whole oral-cavity Dmean decreased in five of seven paired comparisons, and contralateral parotid Dmean decreased in all three detailed pairs. In patient 12, the concurrent reductions in whole and uninvolved oral-cavity Dmean strengthen the evidence for a benefit extending beyond the composite contour that includes the target. The 5.2-Gy and 3.3-Gy reductions

represent 9.3% and 7.3% of the corresponding without-stent doses. These are descriptive patient-specific effects; the small series does not establish a population-level benefit or a reduction in toxicity.

The biological rationale for reducing exposure of uninvolved oral tissues is supported by clinical literature on oral positioning stents. In an observational cohort of 462 oropharyngeal cancer survivors, stent use was associated with less severe selected long-term symptoms, with effects differing by stent type and irradiation volume [11]. This supports the clinical relevance of investigating tissue displacement, but does not establish the same outcomes in the present heterogeneous series. Here, the directly measured advantage is the dosimetric change; prospective assessment of mucositis, salivary function, swallowing, and patient-reported outcomes is needed to determine its clinical benefit.

A scoping review by da Silva Figueiredo et al. identified differences in device design and materials and found that none of the studies assessed had a low risk of bias [12]. In a prospective comparison, Zaid et al. reported noninferiority of printed stents to manually fabricated stents on patient-reported outcomes [13]. The present series documents fitting and continued use. Its routine clinical records do not provide standardized scores for comparing comfort or symptom relief.

For pair 3, the 70-Gy prescription places the uninvolved oral-cavity and mandibular maxima of 73.1 and 73.0 Gy at approximately 104% of prescription. The uninvolved oral cavity was defined as oral cavity minus PTV. This removes geometric overlap but creates no physical separation from the target boundary, so high local doses can persist despite a reduction in mean dose. The essentially unchanged oral-cavity Dmax therefore does not negate the observed 3.3-Gy reduction in its uninvolved mean dose: the two metrics describe different aspects of exposure. Mandibular Dmax should be considered together with the irradiated bone volume and full dose–volume distribution when assessing osteoradionecrosis risk [14].

The ipsilateral submandibular Dmean of 70.0 Gy represents a limitation of organ sparing in this configuration. Published dose–response data associate mean submandibular doses above approximately 39 Gy with marked functional loss and limited recovery [15]. The present findings support selective oral-cavity and parotid dose reduction rather than preservation of all salivary structures. The rise in ipsilateral submandibular dose and mandibular maximum remains part of the overall benefit–risk assessment.

The paired comparison used the same irradiation parameters, with the plan optimized on the with-stent CT and recalculated on the without-stent CT. The observed changes are therefore compatible with dose redistribution associated with tissue positioning and contour differences rather than a change in the prescribed dose. This provides a controlled comparison of anatomical configurations under fixed delivery parameters, but does not establish superiority over a separately optimized without-stent plan. Reported PTV V95% and V100% were unchanged, HI_ratio was unchanged or slightly lower, and CI_95 was slightly higher with the stent. Together, these findings support selective OAR dose reduction without an observed deterioration in the reported target metrics. They do not establish optimal target coverage, statistical superiority, or an unavoidable trade-off in the organs whose doses increased.

The direction of tongue displacement and the degree of mouth opening are determined by the target location, the anatomical conditions for support, and the patient's functional capabilities. The relevance of mouth opening to dosimetric outcomes was examined by Nakazawa et al. [16]. In tumors of the tongue or floor of the mouth, particular attention is given to the relationship between the target and organs at risk, because tongue displacement may also alter the position of the target itself.

In patient 12, the measured palate-to-target distance increased from 7.5 to 15.1 mm on paired planning CT scans, and both the whole and uninvolved oral-cavity mean doses decreased. This observation is consistent with repositioning tissues relative to the dose gradient. It does not quantify the dose to the palate or establish that the same separation was maintained at every fraction.

Recalculation of a single plan on two CT configurations characterizes the dosimetric changes associated with tissue positioning. Qualitative serial kV-CBCT images at fractions 1, 10, 28, and 30 showed broadly similar jaw opening and tongue–palate separation at those fractions. Quantitative assessment of interfraction positioning would complement these observations and permit a more detailed comparison with published findings on digitally fabricated stents [17]. The reported dosimetric endpoints describe dose changes in the selected organs listed in Table 4.

Reproducible Seating and Stabilization of Tissues

The intended mechanical function of the stent is to provide a repeatable reference for the mandibular position and a defined surface against which the displaced tissue rests. In dentate regions, individualized tooth impressions guide seating; in edentulous regions, the available alveolar and mucosal contours provide support. In the present workflow, these relationships are recorded during functional molding and transferred to the printed device. Stable seating provides the mechanical basis for repeatable tissue displacement.

Herpel et al. quantified reinsertion reproducibility using 10 repeated optical scans in one fully dentate volunteer and reported a mean geometric deviation of 98.1 ± 29.4 µm root mean square [2]. This result concerns their tooth-supported device and measured maxillomandibular relationship; it cannot be transferred directly to our PLA stents, edentulous support conditions, or internal soft tissue motion. Doi et al. compared 183 setup observations in six patients using stents with 386 observations in 12 patients without stents and found smaller anterior–posterior and three-dimensional setup errors with stent use [18]. These findings support the positioning rationale, while distinguishing overall setup accuracy from the reproducibility of an individual tissue contour.

Bø et al. evaluated tongue–palate separation using planning CT and daily cone-beam CT and generally found small interfraction variation; one patient showed greater variation associated with incorrect stent orientation [19]. Their observations emphasize the importance of checking insertion orientation and seating during treatment. Our serial images are consistent with maintenance of a similar configuration at selected fractions. Future evaluation should measure jaw and tongue displacement separately on registered volumetric images and assess changes in fit during treatment.

Material and Printed Structure

The radiological characteristics of the stent should be considered in relation to its internal structure. The combination of an outer shell, solid layers, and sparse gyroid infill produces a device containing both polymer elements and air spaces. The 8% infill value refers to the internal structure setting in the slicing software. The combination of polymer and air, together with partial volume effects, may explain the low mean HU values and their variability.

Kunert et al. described the dependence of the X-ray characteristics of printed materials on their structure [20], while Van der Walt et al. investigated the properties of PLA in the context of external beam radiotherapy [21]. In the present approach, the main functional effect of the stent is associated with tissue positioning. Further standardized assessment of CT characteristics and dose perturbations will provide a more detailed account of the contributions of the material and printing parameters. The material documentation concerns migration of selected elements from tested PLA samples and emissions from a specified printer–filament combination. These material-level results and the observed clinical tolerability address different aspects of device performance. Biological safety of the finished, processed and sterilized stent for repeated intraoral contact requires device-level assessment; clinical tolerability alone does not establish it.

Directions for Further Research

This retrospective case series provides descriptive evidence of fabrication, clinical use, and selective dosimetric benefit. The small heterogeneous cohort and seven paired dose comparisons limit generalizability. The fixed-plan recalculation isolates dose redistribution under unchanged delivery parameters; it does not compare independently optimized treatment strategies. Clinical tolerability was described from routine records. Prospective studies using standardized toxicity and patient-reported outcome measures are needed to establish the clinical effects of the observed dose changes.

Further clinical evaluation will combine objective assessment of mucosal reactions with patient-reported symptoms and clearly defined treatment and post-treatment assessment points. This will allow the relationship between tissue positioning, individual dose changes, and clinical outcomes to be investigated.

A promising direction is the inclusion of functional outcomes and quality-of-life measures. Stieb et al. reported an association between stent use and less severe long-term disturbances of taste and appetite after unilateral irradiation, and fewer difficulties with swallowing and chewing after bilateral irradiation [11]. In future work, we plan to combine mucosal assessment with standardized evaluation of swallowing, chewing, taste perception, and patient-reported comfort.

Lee et al. described a randomized comparison of customized printed stents and standard care with clinician-rated mucositis and patient-reported symptoms as primary endpoints [22]. Their 2026 conference abstract

described the study design without reporting outcome data. In our series, the calculated dose changes provide a rationale for measuring these clinical outcomes prospectively.

This retrospective descriptive series characterizes the practical applicability of the workflow, its fabrication characteristics, and initial dosimetric findings. The study is ongoing, with expansion of the sample and continued collection of clinical and dosimetric data. In the next phase, we plan to compare patient-specific intraoral stents with a standard cork stent. The planned comparison will assess dosimetric parameters, positioning reproducibility, and clinical tolerability. Prospective follow-up will allow investigation of the relationship between individual dose changes and the incidence and severity of local reactions, accounting for tumor location and concomitant treatment.

Conclusions

The hybrid workflow of functional molding, optical scanning, and three-dimensional printing enables the fabrication of patient-specific intraoral positioning stents tailored to the patient's anatomy and clinical objectives. In a series of 16 patients, its application was demonstrated for positioning the tongue, lips, and cheek, including in patients with complete edentulism and postoperative anatomical changes. Its main advantages are clinical customization of support, digital reproduction of the device, and the possibility of refabrication from a stored model.

Across seven paired comparisons, mean whole oral-cavity dose decreased from 44.11 to 42.94 Gy, with reductions in five pairs and a maximum reduction of 5.2 Gy. Patient 12 also showed a 3.3-Gy reduction in uninvolved oral-cavity mean dose. In the three detailed pairs, reported target coverage was maintained and conformity at the 95% isodose was slightly greater with the stent. These fixed-plan comparisons illustrate how repositioning tissue can lower the calculated dose to selected structures. The benefit must be assessed alongside increased doses in some adjacent organs. Prospective studies with independently optimized comparator plans, quantitative positioning assessment, and clinical toxicity endpoints are needed to establish the magnitude and clinical value of these effects.

List of abbreviations

CBCT, cone-beam computed tomography; CI, conformity index; CT, computed tomography; Dmax, maximum dose; Dmean, mean dose; DVH, dose-volume histogram; FDM, fused deposition modeling; HI, homogeneity index; HPV, human papillomavirus; HU, Hounsfield units; MDT, multidisciplinary team; OAR, organ at risk; PLA, polylactic acid; PTV, planning target volume; SCC, squamous cell carcinoma; TPS, treatment planning system; VMAT, volumetric modulated arc therapy; XVMC, X-ray Voxel Monte Carlo.

Declarations

Ethics approval and consent to participate

This study was conducted in accordance with the Declaration of Helsinki. The Ethics Commission of the State Non-Commercial Enterprise National Cancer Institute, Ukraine, issued a favourable opinion on the planning of the study entitled “Individual Intraoral Positioning Stents: Hybrid Fabrication and Clinical Verification” and approved the use of the reviewed study materials at the National Cancer Institute (extract from meeting protocol No. 318/2, dated 20 October 2026). This decision also covers the retrospective analysis of clinical data collected before 20 October 2026.

Informed consent was obtained from all patients for participation and clinical use of the patient-specific intraoral stents.

Consent for publication

Consent for publication of the individual clinical details and images included in this article was obtained.

Availability of data and materials

The patient-level characteristics and detailed dosimetric results reported in this study are provided in Tables 1–4. Additional file 1 contains the seven reported paired oral-cavity mean dose changes. The individual clinical records and original imaging datasets are not included in these files. Queries about the underlying data can be addressed to the corresponding author.

Competing interests

The authors declare no conflicts of interest.

Funding

This study received no funding.

Authors' contributions

AD — study conceptualization and initiation of the proposed approach in Ukraine; participation in the study; design and fabrication of patient-specific intraoral positioning stents. Corresponding author.

OB — definition of clinical objectives and stent requirements for the maxillofacial prosthodontic team; participation in the study; clinical follow-up and monitoring of patients during radiotherapy.

DS — participation in the study; development of radiotherapy treatment plans and dosimetric calculations; medical physics support for the study.

NY — definition of clinical objectives and stent requirements for the maxillofacial prosthodontic team; advisory support for the research team.

MS — contribution to study conceptualization; mentoring and advisory support for the research team.

OK — scientific supervision and specialist guidance from a surgical oncology perspective.

RDCP — methodological advice on study design and the selection of required measurements.

RP — methodological guidance on study design and research methods.

RSG — methodological advice on study design and the selection of required measurements.

DF — development of a new approach to stent design and fabrication; participation in the study; scientific supervision.

Acknowledgements

The authors thank the patients who participated in this study.

Authors' information

Anna Dovhan. Dental resident at the Educational and Research Institute of Dentistry, Bogomolets National Medical University; affiliated with the Center for Head and Neck Pathology, Kyiv Regional Clinical Hospital, Kyiv, Ukraine. ORCID: https://orcid.org/0009-0004-7515-188X

Olena Bakhmatska. Senior physician in radiation oncology at the Center for Radiology and Radiation Therapy, National Cancer Institute, Kyiv, Ukraine. ORCID: https://orcid.org/0009-0001-5591-3152

Denys Sliusarenko. Radiology engineer, second qualification category, at the Center for Radiology and Radiation Therapy, National Cancer Institute, Kyiv, Ukraine. ORCID: https://orcid.org/0009-0009-1802-5859

Nadiia Yaroshenko. Head of the Department of Radiation Therapy, National Cancer Institute, Kyiv, Ukraine. ORCID: https://orcid.org/0009-0009-9002-6434

Maryna Sokolovska, PhD. Associate Professor, radiation oncologist, and Head of the Center for Radiation Oncology, National Cancer Institute, Kyiv, Ukraine. Member of the Ministry of Health of Ukraine Working Group on Oncology Care. ORCID: https://orcid.org/0000-0002-7642-7209

Oleg Kravets, DSc. Senior Researcher and Head of the Research and Clinical Department of Head and Neck Tumors, National Cancer Institute, Kyiv, Ukraine. ORCID: https://orcid.org/0000-0002-0226-6238

Ruben Del Castillo Pacora. Radiation oncologist, Department of Oncology, Kingston Health Sciences Centre, Kingston, Ontario, Canada. Assistant Professor, Queen's University, Kingston, Ontario, Canada. ORCID: https://orcid.org/0000-0002-8198-7382

Roman Palyvoda, PhD. Academic Secretary of Bogomolets National Medical University and its Academic Council; Associate Professor in the Department of Maxillofacial Surgery, Educational and Research Institute of Dentistry, Bogomolets National Medical University, Kyiv, Ukraine. ORCID: https://orcid.org/0000-0001-7489-7170

Rodrigo Salazar-Gamarra, MSc, PhD. Dentist and specialist in oral rehabilitation from "Universidade Paulista", Brazil. Professor and Coordinator of the "Unidad de Innovación y Desarrollo en Estomatología" at "Universidad Peruana Cayetano Heredia", Lima, Peru; Coordinator of Research and Development at "Instituto Mais Identidade", São Paulo, Brazil. ORCID: https://orcid.org/0000-0003-2562-9422

Dmytro Filonenko. Maxillofacial prosthodontist and Assistant Lecturer in the Department of Maxillofacial Surgery, Educational and Research Institute of Dentistry, Bogomolets National Medical University, Kyiv, Ukraine. ORCID: https://orcid.org/0009-0000-6738-5724

References

1. Appendino P, Della Ferrera F, Nassisi D, Blandino G, Gino E, Solla SD, et al. Are intraoral customized stents still necessary in the era of Highly Conformal Radiotherapy for Head & Neck cancer? Case series and literature review. Rep Pract Oncol Radiother. 2019;24(5):491–498. https://doi.org/10.1016/j.rpor.2019.07.012

2. Herpel C, Schwindling FS, Held T, Christ L, Lang K, Schwindling M, et al. Individualized 3D-Printed Tissue Retraction Devices for Head and Neck Radiotherapy. Front Oncol. 2021;11:628743. https://doi.org/10.3389/fonc.2021.628743

3. Wilke CT, Zaid M, Chung C, Fuller CD, Mohamed ASR, Skinner H, et al. Design and fabrication of a 3D-printed oral stent for head and neck radiotherapy from routine diagnostic imaging. 3D Print Med. 2017;3:12. https://doi.org/10.1186/s41205-017-0021-4

4. Zaid M, Bajaj N, Burrows H, Mathew R, Dai A, Wilke CT, et al. Creating customized oral stents for head and neck radiotherapy using 3D scanning and printing. Radiat Oncol. 2019;14:148. https://doi.org/10.1186/s13014-019-1357-2

5. Li S, Pang G, Li R, Shi Q, Xu Y, Lu Y, et al. Comparison of custom-designed oral stents in radiotherapy for head and neck malignancies. Front Bioeng Biotechnol. 2025;13:1544105. https://doi.org/10.3389/fbioe.2025.1544105

6. Bruno JS, Miranda-Silva W, Guedes VDS, Parahyba CJ, Moraes FY, Fregnani ER. Digital workflow for producing oral positioning radiotherapy stents for head and neck cancer. J Prosthodont. 2020;29:448–452. https://doi.org/10.1111/jopr.13155

7. Dağdelen M, Dikmen S, Çavdar Karaçam S, Tunçman Kayaokay D, Amasya H, Yolcu MB, et al. Design, fabrication, and clinical dosimetry evaluation of a patient-specific 3D-printed intraoral stent for edentulous head and neck cancer radiotherapy: a prototype dosimetric study. Radiat Phys Chem. 2026;241:113506. https://doi.org/10.1016/j.radphyschem.2025.113506

576 8. Paddick I. A simple scoring ratio to index the conformity of radiosurgical treatment plans. Technical note. J
577 Neurosurg. 2000;93 Suppl 3:219–222. PMID: 11143252.

578 9. International Commission on Radiation Units and Measurements. Prescribing, Recording, and Reporting
579 Photon-Beam Intensity-Modulated Radiation Therapy (IMRT). ICRU Report 83. J ICRU. 2010;10(1). Section
580 3.7.1.

581 10. Tino R, Roach MA, Fuentes GD, Agrawal A, Zaid M, Cooper DJ, et al. Development and clinical
582 implementation of a digital workflow utilizing 3D-printed oral stents for patients with head and neck cancer
583 receiving radiotherapy. Oral Oncol. 2024;157:106944. https://doi.org/10.1016/j.oraloncology.2024.106944

584 11. Stieb S, Perez-Martinez I, Mohamed ASR, Rock S, Bajaj N, Deshpande TS, et al. The impact of tongue-
585 deviating and tongue-depressing oral stents on long-term radiation-associated symptoms in oropharyngeal
586 cancer survivors. Clin Transl Radiat Oncol. 2020;24:71–78. https://doi.org/10.1016/j.ctro.2020.05.014

587 12. da Silva Figueiredo LSP, Souza EG, do Nascimento CD, Gomes GH, Lund RG, Piva E. Materials and
588 effects of intraoral device technologies for complication protection in head and neck cancer radiotherapy: a
589 scoping review. BMC Oral Health. 2025;25:559. https://doi.org/10.1186/s12903-025-05800-1

590 13. Zaid M, Koay EJ, Bajaj N, Mathew R, Xiao L, Agrawal A, et al. A prospective parallel design study
591 testing non-inferiority of customized oral stents made using 3D printing or manually fabricated methods. Oral
592 Oncol. 2020;106:104665. https://doi.org/10.1016/j.oraloncology.2020.104665

593 14. MD Anderson Head and Neck Cancer Symptom Working Group. Dose-volume correlates of mandibular
594 osteoradionecrosis in oropharynx cancer patients receiving intensity-modulated radiotherapy: Results from a
595 case-matched comparison. Radiother Oncol. 2017;124(2):232–239.
596 https://doi.org/10.1016/j.radonc.2017.06.026

597 15. Murdoch-Kinch CA, Kim HM, Vineberg KA, Ship JA, Eisbruch A. Dose-effect relationships for the
598 submandibular salivary glands and implications for their sparing by intensity modulated radiotherapy. Int J
599 Radiat Oncol Biol Phys. 2008;72(2):373–382. https://doi.org/10.1016/j.ijrobp.2007.12.033

16. Nakazawa K, Nakajima J, Ishizaki K, Nomura T, Ueda T. Consideration of mouth opening when using positioning stents during radiotherapy for tongue cancer: a retrospective study. Rep Pract Oncol Radiother. 2022;27:982–989. https://doi.org/10.5603/RPOR.a2022.0107

17. Ma J, Chen Z, Liu S, Hu W, Su K, He R, et al. The application of 3D-printed oral stents in intensity-modulated radiotherapy for oropharyngeal cancer and their dosimetric effect on organs at risk. Eur J Med Res. 2023;28:367. https://doi.org/10.1186/s40001-023-01333-x

18. Doi H, Tanooka M, Ishida T, Moridera K, Ichimiya K, Tarutani K, et al. Utility of intraoral stents in external beam radiotherapy for head and neck cancer. Rep Pract Oncol Radiother. 2017;22(4):310–318. https://doi.org/10.1016/j.rpor.2017.03.002

19. Bø B, Furre T, Dale E. Radiotherapy of tongue cancer using an intraoral stent: a pilot study. J Radiother Pract. 2022;21(3):370–376. https://doi.org/10.1017/S1460396921000078

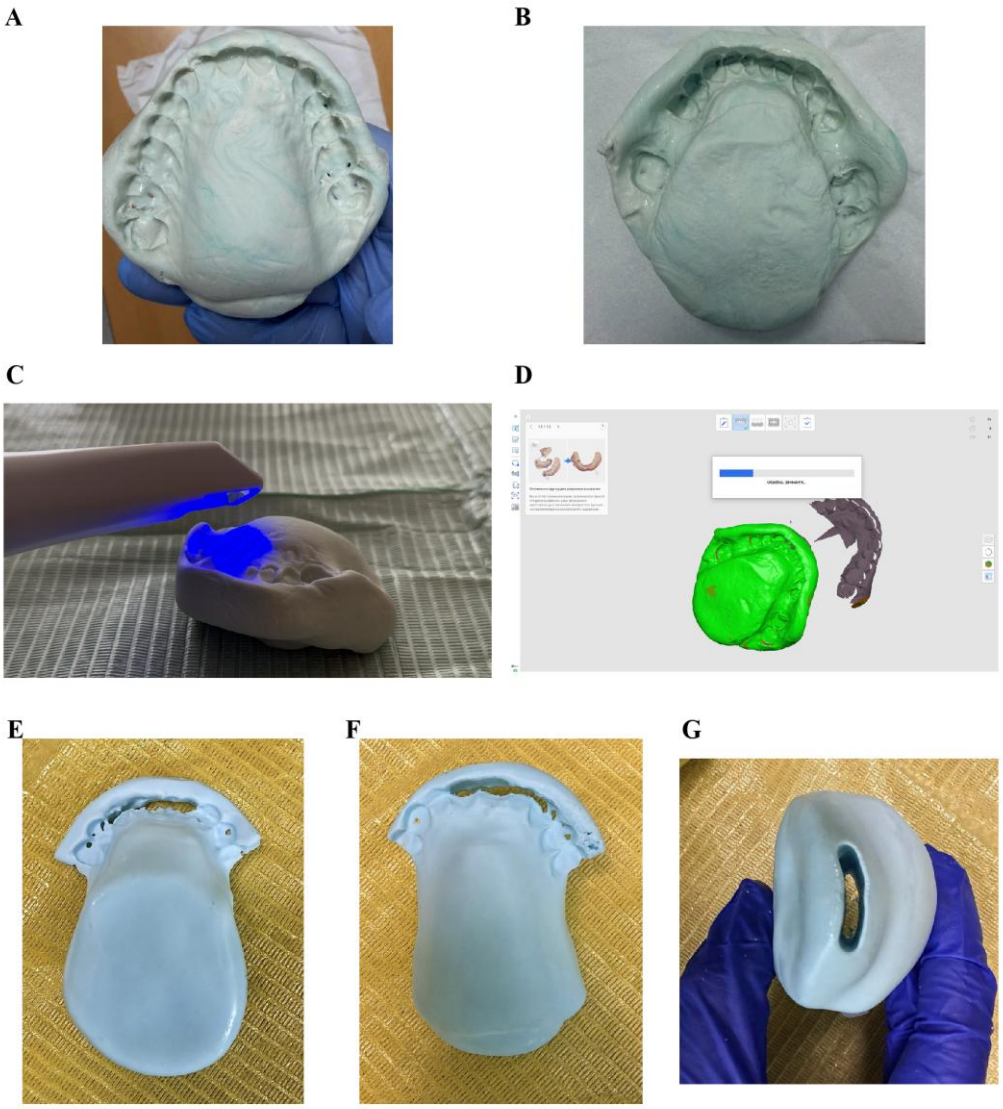
20. Kunert P, Trinkl S, Giussani A, Reichert D, Brix G. Tissue equivalence of 3D printing materials with respect to attenuation and absorption of X-rays used for diagnostic and interventional imaging. Med Phys. 2022;49(12):7766–7778. https://doi.org/10.1002/mp.15987

21. Van der Walt M, Crabtree T, Albantow C. PLA as a suitable 3D printing thermoplastic for use in external beam radiotherapy. Australas Phys Eng Sci Med. 2019;42(4):1165–1176. https://doi.org/10.1007/s13246-019-00818-6

22. Lee A, Tino R, Roach M, Fuentes G, Agrawal A, Zaid M, et al. A randomized study of head and neck radiotherapy with or without customized 3D printed oral stents [conference abstract]. Int J Radiat Oncol Biol Phys. 2026;126(1 Suppl):e702. https://doi.org/10.1016/j.ijrobp.2026.06.2176

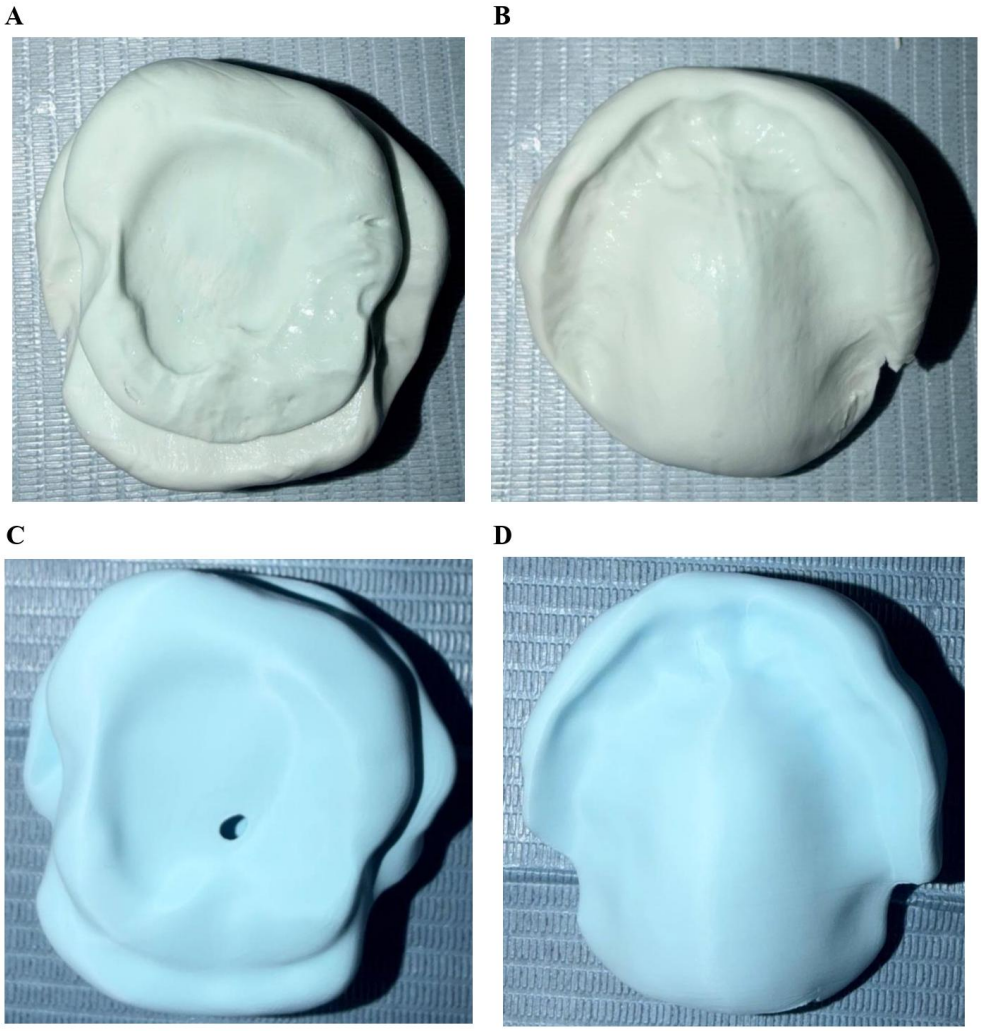
Figures and legends

Figure 1. Silicone pattern, extraoral scanning, and the finished intraoral stent



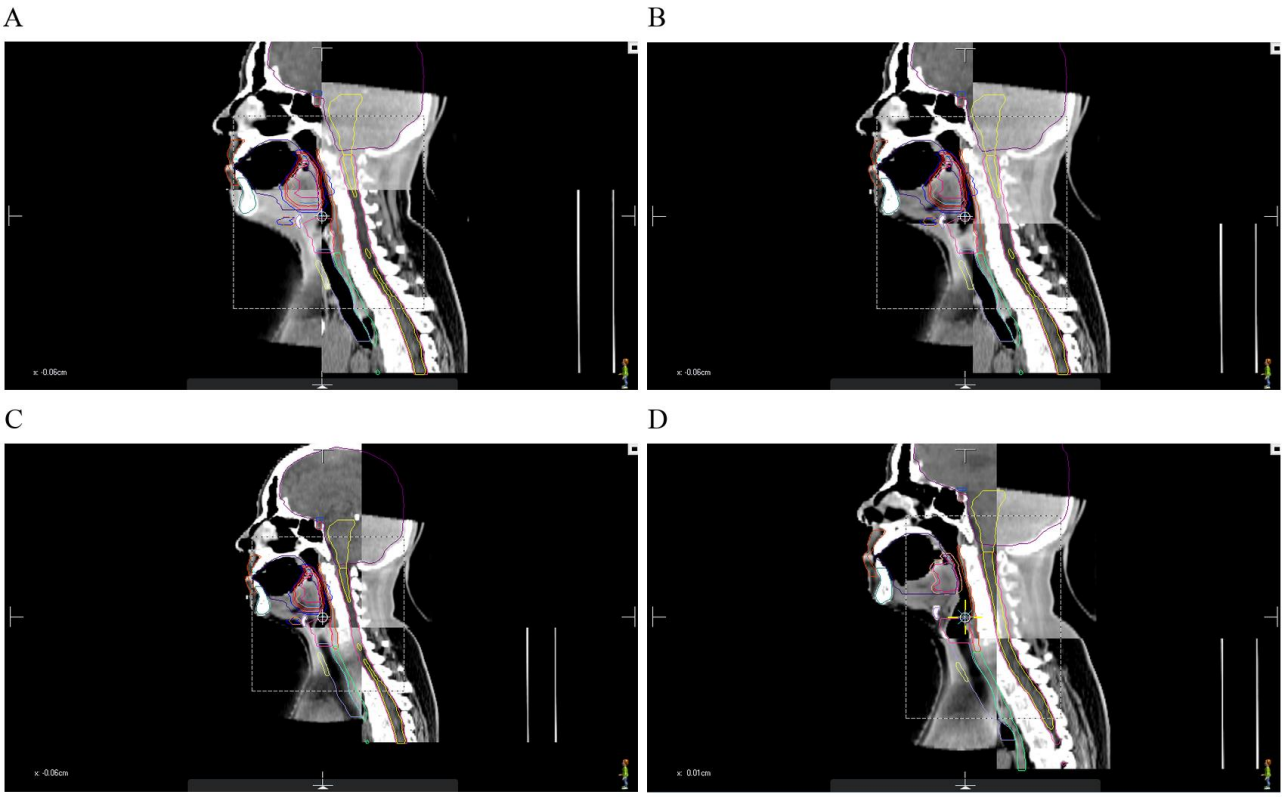
A and B show the palatal and lingual surfaces of the silicone pattern molded in the mouth. C shows the optical scanner digitizing the pattern outside the mouth. D shows digital processing of the scanned geometry. E and F show the lingual and palatal surfaces of the finished printed stent. G shows the breathing channel from the distal end.

Figure 2. Silicone pattern and printed stent for a patient with complete edentulism



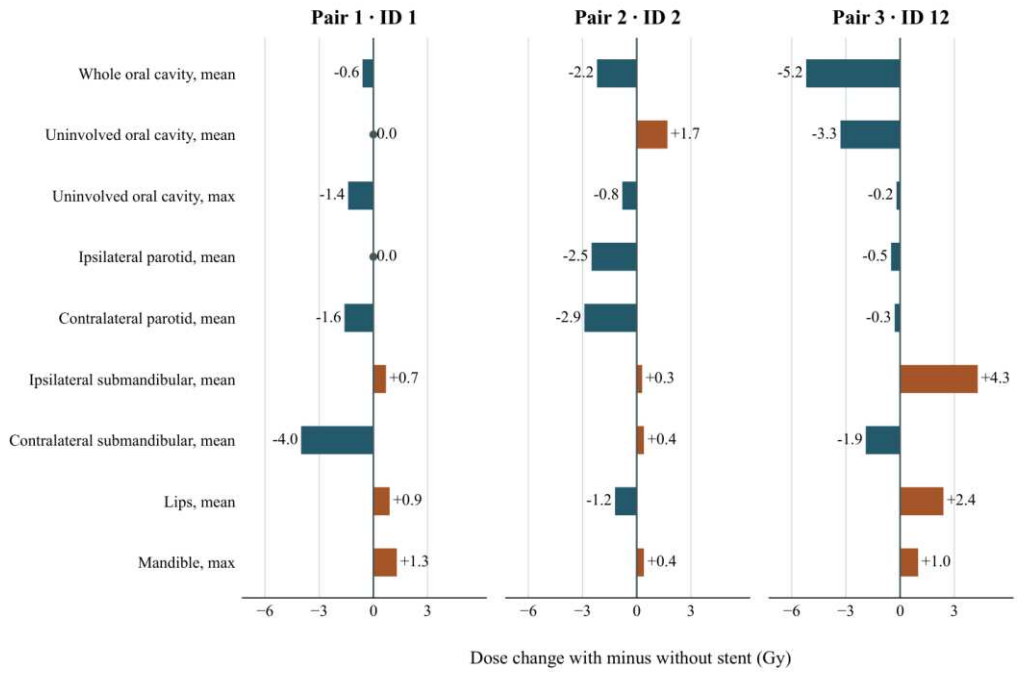
Patient 7 had complete edentulism in both arches and had undergone resection and reconstruction of oral tissues. A and B show the contact surfaces of the functional silicone pattern. C and D show the corresponding surfaces of the printed stent. The broad contact areas follow the available anatomical support.

Figure 3. Jaw opening and tongue–palate separation across four fractions in patient S1



A–D: serial sagittal kV-CBCT images from illustrative patient S1 at fractions 1, 10, 28, and 30, retaining the panel arrangement of the source images. Qualitative review showed broadly similar jaw opening and tongue–palate separation at the displayed fractions.

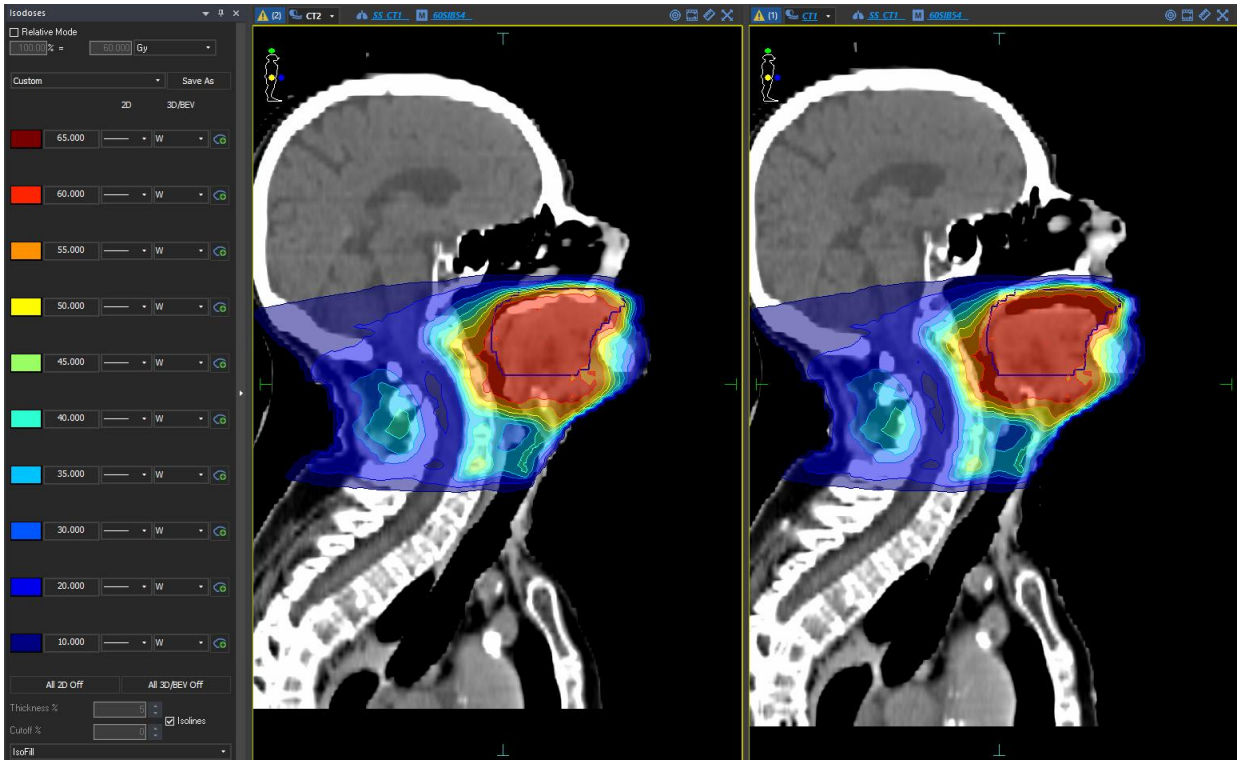
Figure 4. Organ dose changes and target coverage in three paired comparisons



Without → with stent	Pair 1 · ID 1	Pair 2 · ID 2	Pair 3 · ID 12
PTV V95% (%)	100.0 → 100.0	100.0 → 100.0	100.0 → 100.0
PTV V100% (%)	90.0 → 90.0	90.0 → 90.0	90.0 → 90.0
Paddick CI at 95%	0.90 → 0.92	0.87 → 0.89	0.89 → 0.90
HI (D2% / D98%)	1.05 → 1.05	1.06 → 1.05	1.05 → 1.05

Pairs 1-3 correspond to patients 1, 2, and 12, respectively. Bars show the calculated dose with the stent minus the dose without it (Gy). Negative values indicate lower doses with the stent. All three panels use the same scale. The table below the panels shows planning target volume coverage and the conformity and homogeneity indices. Absolute organ doses are reported in Table 4.

Figure 5. Paired sagittal isodose distributions in patient 12



Planning CT without the stent (CT2, left) and with the stent (CT1, right) in dosimetric pair 3. The color key shows the displayed isodose levels in Gy. Table 4 reports the corresponding whole oral-cavity mean doses.

Tables

Table 1. Characteristics of the case series of 16 patients

Characteristic	Value
Number of patients	16
Male / female	9 / 7
Recorded age, median (quartiles), years	56.5 (51.5–74.0)
Recorded age, range, years	41–79
Previous oncological surgery	6 / 16
Caudal tongue displacement	13 / 16
Lip retraction	2 / 16
Cheek retraction	1 / 16
Complete edentulism in both jaws	2 / 16
Tumor site: Base of tongue	5
Tumor site: Lateral tongue	5
Tumor site: Floor of mouth	3
Tumor site: Lower lip	2
Tumor site: Buccal mucosa	1
Completed radiotherapy course with stent	11 / 16
Discontinued use: death / illness	1 / 1
Cases with a summarized treatment-course outcome	13 / 16
Reported breakage / intolerance / device-related pain	0 / 0 / 0
Pre-treatment stent rework for comfort, n	1
Pronounced gag reflex during stent use	0
Pronounced trismus during stent use	0
Adjustment timing	Initial fitting only
Concurrent chemotherapy among eight cases with a yes/no entry: yes / no	6 / 2

Tumor sites follow the principal diagnosis in the clinical registry. Treatment-course outcomes are summarized for 13 patients; concurrent chemotherapy yes/no status is summarized for eight patients. Device tolerability reflects the clinical records. Lack of device-related pain does not imply absence of radiotherapy-related mucositis or other symptoms.

653 **Table 2. Individual tumor diagnoses and selected treatment characteristics**

ID	Tumor site	Histology / HPV status	Recorded TNM and stage	Treatment and prescription recorded
1	Base of tongue	SCC; HPV-unassociated	cT4aN0M0; stage III* (AJCC 8 recorded)	Definitive RT; no prior tumor surgery. MDT prescription: 66 Gy in 33 fractions (2 Gy/fraction); stent used in all 33 fractions. Concurrent cisplatin 100 mg/m² every 21 days.
2	Base of tongue	SCC; HPV-associated	T3N2M0; stage II (AJCC 8 recorded)	Definitive RT; no prior tumor surgery. Prescribed main-target dose 66 Gy in 33 fractions (2 Gy/fraction). Concurrent cisplatin 100 mg/m² every 21 days.
3	Floor of mouth	SCC, G1	T3N2cM0; stage IVA	Definitive RT; no prior tumor surgery. Prescribed 70 Gy in 35 fractions (2 Gy/fraction). Concurrent carboplatin 100 mg/m² every 21 days, as recorded. Course not completed: patient died.
4	Left lateral tongue	SCC	pT3 pN0(0/18) cM0; LV1, Pn1, R0; stage III	Postoperative adjuvant RT: tumor bed 60 Gy (2 Gy/fraction); bilateral neck 50 Gy (1.67 Gy/fraction). 30 fractions recorded. No concurrent chemotherapy.
5	Lower lip vermilion	SCC	cT2N1M0; stage III	Definitive RT; no prior tumor surgery. Prescribed 66 Gy in 33 fractions (2 Gy/fraction). No concurrent chemotherapy.
6	Right lateral tongue	SCC, G2	pT3 pN0(0/24) M0; Pn0, LV0*, R1; stage III	Postoperative adjuvant RT: tumor bed 66 Gy (2 Gy/fraction); neck 50 Gy (1.5 Gy/fraction), as recorded. 33 fractions recorded. Concurrent cisplatin 100 mg/m² every 21 days.
7	Floor of mouth	SCC	pT4a pN1(1/13) cM0; LV1, Pn1, R1; DOI >10 mm; stage IVA	Prior surgery. 33 fractions recorded. Concurrent cisplatin 100 mg/m² every 21 days.
8	Right base of tongue	SCC; HPV-associated	cT2N2M0; stage II	No prior tumor surgery. Prescribed 66 Gy in 33 fractions (2 Gy/fraction). Three prior DCF cycles; concurrent cisplatin 100 mg/m² every 21 days.

ID	Tumor site	Histology / HPV status	Recorded TNM and stage	Treatment and prescription recorded
9	Left base of tongue	SCC; HPV-associated	cT2 cN3 M0; stage IVB*	Three prior induction DCF cycles, with clinical complete response recorded.
10	Right floor-of-mouth mucosa	SCC	cT4aN2bM0; stage IVA	RT discontinued because of peritonitis and pneumonia.
11	Left lateral tongue	SCC, G1	T2N2bM0; stage IVA	Definitive RT; no prior tumor surgery. Prescribed 70 Gy in 35 fractions (2 Gy/fraction). Concurrent carboplatin 100 mg/m² every 21 days.
12	Left lateral tongue; base of tongue / oropharynx also recorded*	Keratinizing SCC, G2; HPV-unassociated; p16-negative	pT3 pN1(1/10) M0; LV1, Pn1, R0; DOI >10 mm (AJCC 8 recorded)	Postoperative adjuvant RT. Main-target prescription: 70 Gy.
13	Left buccal mucosa	Keratinizing SCC	Initial cT4aN2cM0, stage IVA; postoperative ypT2 pN0(0/24), LV0, Pn0, R0	Three prior combination chemotherapy cycles plus cetuximab, followed by surgery; 30 fractions recorded.
14	Base of tongue	Invasive SCC, G2, basaloid subtype; HPV testing pending in the record	cT3N0M0; stage III	Definitive RT with cisplatin planned
15	Right lower lip	Invasive SCC	Principal MDT record: cT2 cN1 M0, stage III; T1N0M0 also recorded*	Definitive RT planned after surgery was declined. Proposed tumor dose 60–66 Gy and neck dose 50–54 Gy
16	Left lateral tongue	Keratinizing SCC, G1	pT3 pN0(0/18) M0; LV1, Pn0, R0; DOI >10 mm; stage III	Prior tumor surgery. Postoperative adjuvant RT planned

SCC, squamous cell carcinoma; HPV, human papillomavirus; RT, radiotherapy; DOI, depth of invasion; MDT, multidisciplinary team. An asterisk marks a source entry requiring clarification. Histologic grades and LV, Pn and R descriptors follow the registry. Treatment entries distinguish prescribed or planned regimens from recorded delivery. Patients 1, 2 and 12 correspond to dosimetric pairs 1, 2 and 3, respectively.

Table 3. Printing time and stent mass in the case series

Patient	Time, min	Mass, g	Note
1	170	22.0	
2	195	21.0	
3	175	21.0	
4	180	22.0	
5	93	15.0	
6	145	22.0	
7	132	21.5	
8	165	22.0	
9	162	21.0	
10	230	21.6	Two variants printed simultaneously
11	190	20.5	
12	200	20.5	Two variants printed simultaneously
13	40	12.0	
14	90	19.5	
15	130	21	
16	120	22.0	

Time is per print job. Two variants were printed together for patients 10 and 12. Mass refers to the registry-recorded stent. Print time excludes hands-on work.

Table 4. Paired dosimetric values and changes

Structure or parameter	Pair 1 (ID 1)	Pair 2 (ID 2)	Pair 3 (ID 12)
Entire oral cavity - mean dose	50.6 → 50.0 Δ -0.6	59.9 → 57.7 Δ -2.2	56.2 → 51.0 Δ -5.2
Uninvolved oral cavity - mean dose	38.0 → 38.0 Δ +0.0	54.7 → 56.4 Δ +1.7	45.3 → 42.0 Δ -3.3
Uninvolved oral cavity - maximum dose	73.6 → 72.2 Δ -1.4	64.8 → 64.0 Δ -0.8	73.3 → 73.1 Δ -0.2

Structure or parameter	Pair 1 (ID 1)	Pair 2 (ID 2)	Pair 3 (ID 12)
Ipsilateral parotid gland - mean dose	24.5 → 24.5 Δ +0.0	27.4 → 24.9 Δ -2.5	25.5 → 25.0 Δ -0.5
Contralateral parotid gland - mean dose	24.5 → 22.9 Δ -1.6	26.6 → 23.7 Δ -2.9	22.3 → 22.0 Δ -0.3
Ipsilateral submandibular gland - mean dose	62.7 → 63.4 Δ +0.7	61.5 → 61.8 Δ +0.3	65.7 → 70.0 Δ +4.3
Contralateral submandibular gland - mean dose	61.8 → 57.8 Δ -4.0	55.2 → 55.6 Δ +0.4	60.9 → 59.0 Δ -1.9
Lips - mean dose	12.7 → 13.6 Δ +0.9	32.5 → 31.3 Δ -1.2	14.7 → 17.1 Δ +2.4
Mandible - maximum dose	71.5 → 72.8 Δ +1.3	62.9 → 63.3 Δ +0.4	72.0 → 73.0 Δ +1.0
PTV V95%, %	100.0 → 100.0 Δ +0.0	100.0 → 100.0 Δ +0.0	100.0 → 100.0 Δ +0.0
PTV V100%, %	90.0 → 90.0 Δ +0.0	90.0 → 90.0 Δ +0.0	90.0 → 90.0 Δ +0.0
Paddick conformity index (CI_95)	0.90 → 0.92 Δ +0.02	0.87 → 0.89 Δ +0.02	0.89 → 0.90 Δ +0.01
Homogeneity index (HI_ratio = D2%/D98%)	1.05 → 1.05 Δ +0.00	1.06 → 1.05 Δ -0.01	1.05 → 1.05 Δ +0.00

Entries show without → with stent; Δ = with minus without. Dose in Gy; coverage differences in percentage points. CI_95 and HI_ratio are defined in Methods.

Supplementary Files

This is a list of supplementary files associated with this preprint. Click to download.

- CBCT1.mp4
- CBCT2.mp4
- Additionalfile1.png
- Additionalfile2.pdf